

Old Dominion University ODU Digital Commons

Chemistry & Biochemistry Faculty Publications

Chemistry & Biochemistry

2017

A Nutrient-Regulated Cyclic Diguanylate Phosphodiesterase Controls *Clostridium difficile* Biofilm and Toxin Production During Stationary Phase

Erin B. Purcell
Old Dominion University

Robert W. McKee


David S. Courson
Old Dominion University

Elizabeth M. Garrett

Shonna M. McBride

See next page for additional authors

Follow this and additional works at: https://digitalcommons.odu.edu/chemistry_fac_pubs

 Part of the [Biology Commons](#), and the [Microbiology Commons](#)

Repository Citation

Purcell, Erin B.; McKee, Robert W.; Courson, David S.; Garrett, Elizabeth M.; McBride, Shonna M.; Cheney, Richard E.; and Tamayo, Rita, "A Nutrient-Regulated Cyclic Diguanylate Phosphodiesterase Controls *Clostridium difficile* Biofilm and Toxin Production During Stationary Phase" (2017). *Chemistry & Biochemistry Faculty Publications*. 92.
https://digitalcommons.odu.edu/chemistry_fac_pubs/92

Original Publication Citation


Purcell, E. B., McKee, R. W., Courson, D. S., Garrett, E. M., McBride, S. M., Cheney, R. E., & Tamayo, R. (2017). A nutrient-regulated cyclic diguanylate phosphodiesterase controls *Clostridium difficile* biofilm and toxin production during stationary phase. *Infection and Immunity*, 85(9 (Article e00347)), 1-17. doi:10.1128/IAI.00347-17

Authors

Erin B. Purcell, Robert W. McKee, David S. Courson, Elizabeth M. Garrett, Shonna M. McBride, Richard E. Cheney, and Rita Tamayo



A Nutrient-Regulated Cyclic Diguanylate Phosphodiesterase Controls *Clostridium difficile* Biofilm and Toxin Production during Stationary Phase

Erin B. Purcell,^b Robert W. McKee,^a David S. Courson,^b Elizabeth M. Garrett,^a Shonna M. McBride,^d Richard E. Cheney,^c  Rita Tamayo^a

Department of Microbiology and Immunology, University of North Carolina at Chapel Hill School of Medicine, Chapel Hill, North Carolina, USA^a; Department of Chemistry and Biochemistry, Old Dominion University, Norfolk, Virginia, USA^b; Department of Cell Biology and Physiology, Lineberger Comprehensive Cancer Center, University of North Carolina at Chapel Hill School of Medicine, Chapel Hill, North Carolina, USA^c; Department of Microbiology and Immunology, Emory Antibiotic Resistance Center, Emory University School of Medicine, Atlanta, Georgia, USA^d

ABSTRACT The signaling molecule cyclic diguanylate (c-di-GMP) mediates physiological adaptation to extracellular stimuli in a wide range of bacteria. The complex metabolic pathways governing c-di-GMP synthesis and degradation are highly regulated, but the specific cues that impact c-di-GMP signaling are largely unknown. In the intestinal pathogen *Clostridium difficile*, c-di-GMP inhibits flagellar motility and toxin production and promotes pilus-dependent biofilm formation, but no specific biological functions have been ascribed to any of the individual c-di-GMP synthases or phosphodiesterases (PDEs). Here, we report the functional and biochemical characterization of a c-di-GMP PDE, PdcA, 1 of 37 confirmed or putative c-di-GMP metabolism proteins in *C. difficile* 630. Our studies reveal that *pdcA* transcription is controlled by the nutrient-regulated transcriptional regulator CodY and accordingly increases during stationary phase. In addition, PdcA PDE activity is allosterically regulated by GTP, further linking c-di-GMP levels to nutrient availability. Mutation of *pdcA* increased biofilm formation and reduced toxin biosynthesis without affecting swimming motility or global intracellular c-di-GMP. Analysis of the transcriptional response to *pdcA* mutation indicates that PdcA-dependent phenotypes manifest during stationary phase, consistent with regulation by CodY. These results demonstrate that inactivation of this single PDE gene is sufficient to impact multiple c-di-GMP-dependent phenotypes, including the production of major virulence factors, and suggest a link between c-di-GMP signaling and nutrient availability.

KEYWORDS CodY, biofilm, c-di-GMP, cyclic diguanylate, flagella, flagellar motility, nutrient, toxin

The anaerobic, Gram-positive bacterium *Clostridium difficile* is the most common cause of nosocomial infections in the developed world, resulting in symptoms ranging from mild diarrhea to potentially lethal pseudomembranous colitis (1). *C. difficile* exposure rarely results in symptomatic infections in healthy individuals, as a healthy microbiota creates an environment that hinders *C. difficile* growth (2, 3). The main risk factor for an initial *C. difficile* infection is disruption of the gut microbiota by antibiotic treatment, which creates a transient “nutrient bloom” due to drug-induced disruption of normal bacterial metabolism (4–7).

The *C. difficile* life cycle has two distinct phases with different roles in disease: metabolically active vegetative cells and dormant spores. *C. difficile* spores are resistant to oxygen, heat, and many commercial disinfectants, making their eradication from

Received 12 May 2017 Returned for
modification 6 June 2017 Accepted 20 June
2017

Accepted manuscript posted online 26
June 2017

Citation Purcell EB, McKee RW, Courson DS, Garrett EM, McBride SM, Cheney RE, Tamayo R. 2017. A nutrient-regulated cyclic diguanylate phosphodiesterase controls *Clostridium difficile* biofilm and toxin production during stationary phase. *Infect Immun* 85:e00347-17. <https://doi.org/10.1128/IAI.00347-17>.

Editor Vincent B. Young, University of Michigan—Ann Arbor

Copyright © 2017 American Society for Microbiology. All Rights Reserved.

Address correspondence to Rita Tamayo, rita_tamayo@med.unc.edu.

contaminated environments difficult (8–10). In the anaerobic mammalian intestine, spores germinate into vegetative cells, a process triggered by chemical signals including certain amino acids and bile acids (11, 12). Vegetative *C. difficile* cells secrete protein cytotoxins that drive the development of disease symptoms (13, 14). These cytotoxins, TcdA and TcdB, are internalized by host epithelial cells, where they glucosylate and inactivate the Rho and Rac GTPases that regulate the host actin cytoskeleton (15–18). Intoxication leads to actin depolymerization, with cytopathic effects including cell rounding and disruption of cell-cell tight junctions, which effectively permeabilizes the intestinal epithelium (13, 14, 19). *C. difficile* toxins are capable of inducing apoptosis and necrosis in intoxicated cells (20, 21). The effects of these toxins result in diarrhea and trigger a massive inflammatory response in the host (14, 22, 23).

During infection, *C. difficile* cells can either remain vegetative or differentiate into spores, which are shed in stool and allow transmission of *C. difficile* to new hosts (24). The factors that influence the balance between vegetative growth and sporulation *in vivo* are poorly understood. There is growing evidence that nutrient uptake from the environment inhibits the onset of sporulation, as spore formation is negatively regulated by nutrient transporters (25, 26). In vegetative *C. difficile*, nutrient availability also modulates the activity of CodY, a transcriptional regulator that is conserved among low-GC Gram-positive bacteria. When CodY is activated by binding of branched-chain amino acids (BCAA), it binds to target DNA sequences and primarily represses gene transcription (27). In some organisms, including *C. difficile*, CodY is also activated by GTP (28–30). When BCAA and GTP are abundant, such as in exponential phase, CodY represses the transcription of stationary-phase metabolic genes such as amino acid synthetases and peptide transporters (31, 32). Intracellular stores of BCAA and GTP become limited during stationary phase (28, 33, 34), relieving CodY repression of these genes. In a number of Gram-positive pathogens, including *C. difficile*, *Staphylococcus aureus*, and *Listeria monocytogenes*, CodY represses the transcription of virulence factor genes during exponential growth (30, 35–38). Microarray analysis and affinity purification of CodY binding targets have revealed that CodY regulates the transcription of hundreds of *C. difficile* genes, including some with predicted roles in signaling by the second messenger cyclic diguanylate (c-di-GMP) (27).

In a multitude of Gram-negative bacteria, c-di-GMP regulates transitions between motile, planktonic lifestyles and sessile modes of growth, often involving biofilm formation (39). In several Gram-negative pathogens, c-di-GMP also influences virulence (40–45). The regulatory roles of c-di-GMP in Gram-positive bacteria are less well characterized but appear to be largely conserved with Gram-negative species, with elevated c-di-GMP inhibiting swimming motility and promoting nonmotile lifestyles (46).

c-di-GMP is synthesized from GTP by diguanylate cyclase (DGC) enzymes containing a characteristic GGDEF domain (47) and degraded by two families of phosphodiesterase (PDE) enzymes identified by conserved EAL or HD-GYP domains (48, 49). Bacterial genomes commonly contain multiple genes encoding these domains, which are often coupled to sensory or regulatory domains (50, 51). The *C. difficile* 630 genome encodes 37 DGCs and PDEs (52). The c-di-GMP-metabolizing activity of 28 of these enzymes has been confirmed by heterologous expression in *Vibrio cholerae* and/or *Bacillus subtilis* (53, 54). Elevated cytoplasmic levels of c-di-GMP repress *C. difficile* flagellar biosynthesis and toxin production and enhance type IV pilus biogenesis and biofilm formation (55–60). c-di-GMP also appears to regulate the production of clostridial proteins that interact with the mammalian extracellular matrix, suggesting a role for c-di-GMP in the regulation of adhesion to host cells (56, 61–63). While c-di-GMP regulates multiple processes with a known or potential role in virulence, specific functions have not yet been ascribed to any of the individual *C. difficile* DGCs or PDEs.

In this study, we examined the transcriptional and posttranslational regulation of the *C. difficile* c-di-GMP PDE PdcA and determined its role in the regulation of c-di-GMP-dependent processes. We show that *pdcA* is a stationary-phase gene regulated by CodY and that PdcA enzymatic activity is regulated by GTP via its GGDEF domain,

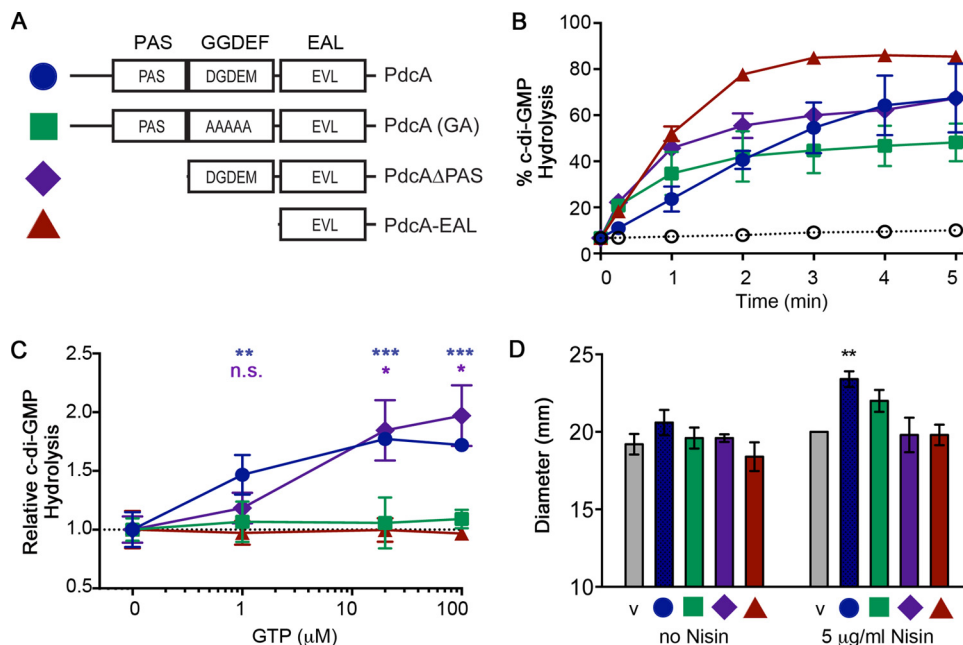


FIG 1 PdcA enzymatic activity is controlled by regulatory domains *in vitro* and *in vivo*. (A) Schematic of the PdcA derivatives used in these experiments with the corresponding domains and colors used in panels B to D. The EAL domain of PdcA contains a substitution of valine for alanine in the EAL motif, noted here as EVL. (B) Percentages of initial c-di-GMP substrate hydrolyzed by full-length PdcA, PdcA(GA), PdcAΔPAS, and PdcA-EAL, determined at 1-min intervals after initiation of the reaction upon addition of the substrate. Open circles indicate values for buffer-only negative controls. The data shown are mean values and standard deviations from three [WT and PdcA(GA)] or two (PdcAΔPAS and PdcA-EAL) separate protein purifications. (C) PDE activity, expressed as a percentage of the starting c-di-GMP hydrolyzed at 1 min with increasing concentrations of GTP. The data shown are mean values and standard deviations. The activity of full-length PdcA (blue) and PdcAΔPAS (purple) at a given GTP concentration was compared to the activity of the same protein in the absence of GTP by one-way analysis of variance (*, $P < 0.05$; **, $P < 0.01$; ***, $P < 0.001$; asterisks are color coded according to comparison). The activities of PdcA(GA) and PdcA-EAL in the presence of GTP were compared to their activities in the absence of GTP by one-way analysis of variance and were not statistically significantly different at any of the GTP concentration tested (not shown). (D) *C. difficile* strains with (left to right) the vector (v), pPdcA, pPdcA(GA), pPdcAΔPAS, or pPdcA-EAL were assayed for motility in BHIS-Tm with 0.3% agar supplemented with 0 or 5 $\mu\text{g/ml}$ nisin. Motility diameters were measured after 72 h at 37°C. Data were analyzed by two-way analysis of variance and Bonferroni's multiple-comparison test comparing values to the average vector control value (**, $P < 0.01$).

indicating that nutrient availability impacts c-di-GMP signaling in *C. difficile*. Notably, mutation of *pdca* impacts multiple c-di-GMP-regulated processes, including biofilm formation and toxin production. Thus, this study identified a single c-di-GMP PDE capable of broadly affecting *C. difficile* c-di-GMP signaling during stationary phase.

RESULTS

The PAS and GGDEF domains affect PdcA function *in vitro* and *in vivo*. We previously reported that full-length PdcA and its EAL domain alone exhibit c-di-GMP PDE activity *in vitro* but that overproduction of the PdcA EAL domain alone had no detectable effect on the cytoplasmic c-di-GMP concentration or flagellar motility of *C. difficile* (55). Heterologous overproduction of full-length PdcA in *V. cholerae* or *B. subtilis* increases motility and decreases *V. cholerae* biofilm formation, consistent with decreased c-di-GMP (53, 54), leading us to hypothesize that the other domains of PdcA are required for activity of the EAL domain *in vivo*. Full-length PdcA is a PAS-GGDEF-EAL fusion protein (Fig. 1A). The PdcA EAL domain contains a valine substitution for the alanine in the canonical EAL motif (i.e., EVL). While the glutamic acid in the EAL sequence is required for PDE activity, the alanine residue has been shown previously to be dispensable (42, 55). The PAS domain is part of a family of regulatory domains that can bind diverse small-molecule ligands and often regulates protein activity through protein-protein interactions (64). The PdcA GGDEF domain contains a degenerate active site (DGDEM) and has been demonstrated to be catalytically inactive (55). In

some homologous proteins with tandem GGDEF-EAL domains, catalytically inactive GGDEF domains are capable of binding GTP, which enhances the PDE activity of the associated EAL domains (65–68). Crystal structures of catalytically active and inactive DGCs suggest that the small side chain of the glycine at position 2 creates a binding pocket for the guanine base of GTP, while the aspartic acid at position 4 coordinates a magnesium ion that interacts with the phosphates (69–71). These residues are conserved in PdcA, suggesting a regulatory role for its GGDEF domain.

To examine the potential regulatory effects of the PAS and GGDEF domains on PdcA enzymatic activity, we analyzed the full-length protein and three derivatives: full-length PdcA in which the putative DGDEM cyclase active-site residues are mutated to alanines [PdcA(GA)], a truncated protein with no N-terminal PAS domain (PdcA- Δ PAS), and the isolated PDE domain (PdcA-EAL) (Fig. 1A). The enzymatic activities of these recombinant proteins, along with wild-type (WT) PdcA, were assayed *in vitro* with radioactive c-di-GMP as a substrate. All of these proteins hydrolyzed c-di-GMP to various degrees (Fig. 1B). To determine whether GTP binding to the GGDEF domain stimulates hydrolytic activity by the EAL domain, we assayed c-di-GMP cleavage in the presence of increasing amounts of GTP. WT PdcA activity was increased 50% by the addition of one molar equivalent of GTP and increased in a dose-dependent manner at higher GTP concentrations (Fig. 1C). PdcA- Δ PAS, which has an intact DGDEM sequence, was less responsive to low levels of GTP than the WT but also displayed a dose-dependent GTP-stimulated increase in PDE activity (Fig. 1C). The enzymatic activities of PdcA(GA) and PdcA-EAL, both of which lack the DGDEM putative GTP-binding motif, were unaffected by GTP (Fig. 1C). The results are consistent with allosteric activation of PDE activity of the EAL domain as a result of GTP binding to the DGDEM sequence in the GGDEF domain, as has been observed for several other tandem GGDEF-EAL proteins with degenerate GGDEF domains (65–68). The PdcA- Δ PAS protein was slightly less active than the full-length protein *in vitro* (Fig. 1B), suggesting an as-yet-undefined regulatory function for the N-terminal PAS domain.

We next evaluated the roles of the PdcA regulatory domains *in vivo* by comparing the effects of overproducing WT PdcA or the PdcA(GA), PdcA- Δ PAS, or PdcA-EAL derivative in *C. difficile*. The genes for these PdcA variants were expressed in *C. difficile* with a plasmid-borne expression system in which sublethal concentrations of the antimicrobial peptide nisin induce gene expression (55). We did not assay biofilm formation in these strains, as the *C. difficile* 630 strain does not form very dense biofilms (60, 72), so the anticipated decreases upon PDE overproduction would likely be subtle. We have previously reported that overproduction of PdcA-EAL does not impact flagellar motility within 96 h (55). Here, *C. difficile* overproducing WT full-length PdcA exhibited a significant, nisin-dependent increase in motility compared to the vector control strain by 72 h, consistent with reduced c-di-GMP upon WT PdcA overproduction (Fig. 1D). Overproduction of PdcA(GA), PdcA- Δ PAS, or PdcA-EAL did not significantly affect motility, indicating that the PAS and GGDEF regulatory domains are necessary for maximal PdcA enzymatic activity *in vivo*.

***pdca* transcription is regulated by CodY.** Previous studies have demonstrated that PdcA, 1 of 19 EAL domain proteins encoded in the *C. difficile* genome, is a functional c-di-GMP PDE (53–55). However, the contribution of PdcA to c-di-GMP signaling in *C. difficile* is unknown. Previous transcriptional profiling studies suggested that *pdca* expression is greater during stationary phase than during exponential growth and is reduced in *C. difficile* lacking SigH, a sigma factor involved in the onset of stationary phase and the initiation of spore formation (73). In addition, a study aimed at identifying DNA sequences bound by the transcription factor CodY in *C. difficile* identified a sequence overlapping the 5' end of the *pdca* coding sequence (CD630_15150) (27, 30). To determine whether *pdca* transcription shows CodY-dependent growth phase regulation, we performed quantitative reverse transcription-PCR (qRT-PCR) to evaluate transcript abundance in *C. difficile* mRNA harvested during exponential-phase and early stationary-phase growth. Two stationary-phase genes previously shown to be regu-

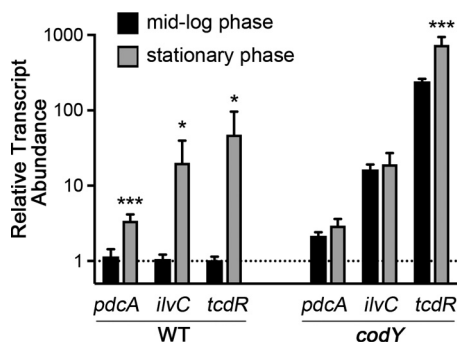


FIG 2 CodY regulates *pdca* transcription. Transcript levels of the genes indicated in WT JIR8094 (erythromycin-sensitive derivative of *C. difficile* strain 630) and an isogenic *codY*-null strain in exponential phase (black) and stationary phase (gray) were measured by qRT-PCR. The data were analyzed by the ΔC_T method as described in Materials and Methods, here with exponential-phase WT cells as the reference condition. The mean values and standard deviations from three biological replicates are shown. The data were analyzed by unpaired *t* test comparing the exponential- and stationary-phase transcript levels of each gene (*, $P < 0.05$; ***, $P < 0.001$).

lated by CodY, *ilvC* and *tcdR*, served as positive controls (30). In WT cells (JIR8084, a derivative of *C. difficile* 630), the *pdca* transcript was three times as abundant in stationary phase as in log phase (Fig. 2). Similar results were obtained for *ilvC* and *tcdR*, which were 12- and 20-fold more abundant during stationary phase, respectively. In a *codY* mutant, transcript levels of *pdca*, *ilvC*, and *tcdR* were higher than in the parent strain (2-, 12-, and 20-fold higher, respectively) during exponential phase, indicating derepression of these genes in the absence of CodY (Fig. 2). Stationary phase onset in the *codY* null strain caused no significant further increase in *pdca* or *ilvC* transcripts, and the *tcdR* transcript showed a modest 3-fold increase (Fig. 2). Thus, expression of all three genes during exponential growth was repressed in WT *C. difficile* and not in the *codY* null strain, indicating that *pdca* is a *bona fide* CodY-regulated gene expressed during stationary phase (27).

Though Dineen et al. identified a DNA region encompassing the *pdca* translational start site by affinity purification with CodY, the putative *pdca* promoter region lacked a recognizable CodY consensus binding sequence by the specified criteria (27, 30). We used electrophoretic mobility shift assays (EMSAs) to determine whether CodY binds *pdca* promoter DNA. We chose a DNA region containing the 194-bp sequence pulled down by CodY, which includes the first 146 bp of the *pdca* coding sequence (27), plus an additional 261 bp of the upstream sequence. GTP and BCAA leucine, isoleucine, and valine, which stimulate CodY binding to target DNA in *C. difficile*, were included in the binding reaction mixtures, and the amino acids were added to the electrophoresis buffer (30). CodY had no effect on the migration of the 133-bp nonspecific, negative control DNA fragment of *V. cholerae gbpA* included in each binding reaction mixture. As shown previously, CodY bound to and shifted the migration of the *ilvC* promoter region, which served as a positive control (Fig. 3A) (27). Similarly, CodY bound to the *pdca* promoter fragment (Fig. 3B). These results suggest that CodY negatively regulates *pdca* transcription by binding directly to the *pdca* promoter.

Mutation of *pdca* specifically affects stationary-phase phenomena. Despite using multiple targeting sequences, we were unsuccessful in generating a *pdca* mutant via insertional inactivation by a targeted intron (74). As an alternative, we replaced the *pdca* open reading frame (ORF) with the *catP* gene by allelic exchange. We cloned the 2,000-bp sequences upstream and downstream of *pdca* into pMC234 flanking the *catP* gene (see Fig. S1 in the supplemental material). The construct was introduced into *C. difficile* 630 by conjugation. After the identification of a thiamphenicol-resistant recombinant strain in which the plasmid had recombined into the chromosome at the *pdca* locus, it was passaged without selection to allow plasmid loss. The resulting thiamphenicol-sensitive isolates were screened by PCR to identify an isolate in

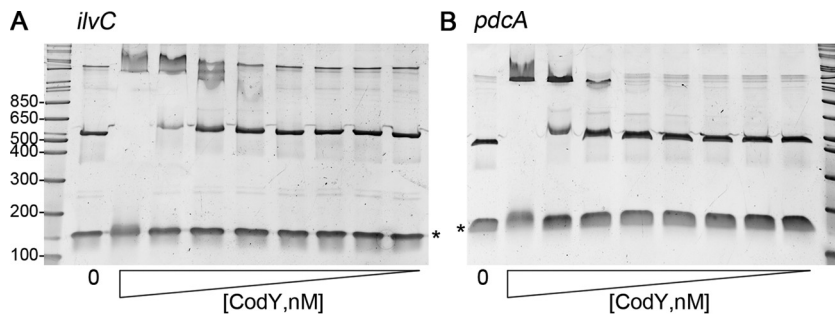


FIG 3 CodY binds directly to the *pdcA* promoter region. Purified six-histidine-tagged *C. difficile* CodY was tested for the ability to bind the *pdcA* promoter region with EMSAs. Serial 2-fold dilutions of CodY were incubated with the *ilvC* promoter region previously shown to be directly bound by CodY (A) or the *pdcA* promoter region (B). As a negative control, a 133-bp *V. cholerae* DNA fragment was included in each binding reaction mixture (asterisks). The concentrations of CodY used were (left to right) 0, 7.2, 3.6, 1.8, 0.9, 0.45, 0.23, 0.12, and 0.06 μ M. In each reaction mixture and in the electrophoresis buffer, isoleucine, leucine, and valine were added to promote CodY binding. A representative of three independent experiments is shown. The values to the left are molecular sizes in kilodaltons.

which *pdcA* had been replaced on the chromosome with *catP* by double homologous recombination (Fig. S1) (75).

The resulting *pdcA::catP* mutant was assessed for altered *c*-di-GMP and related phenotypes, including flagellar motility, biofilm formation, and toxin production (55, 57). The cytoplasmic *c*-di-GMP concentrations of the WT and *pdcA::catP* deletion *C. difficile* strains grown to early stationary phase were assayed by ultraperformance liquid chromatography coupled to mass spectrometry (UPLC-MS) and found to be indistinguishable (Fig. 4A), indicating that the absence of PdcA does not impact global

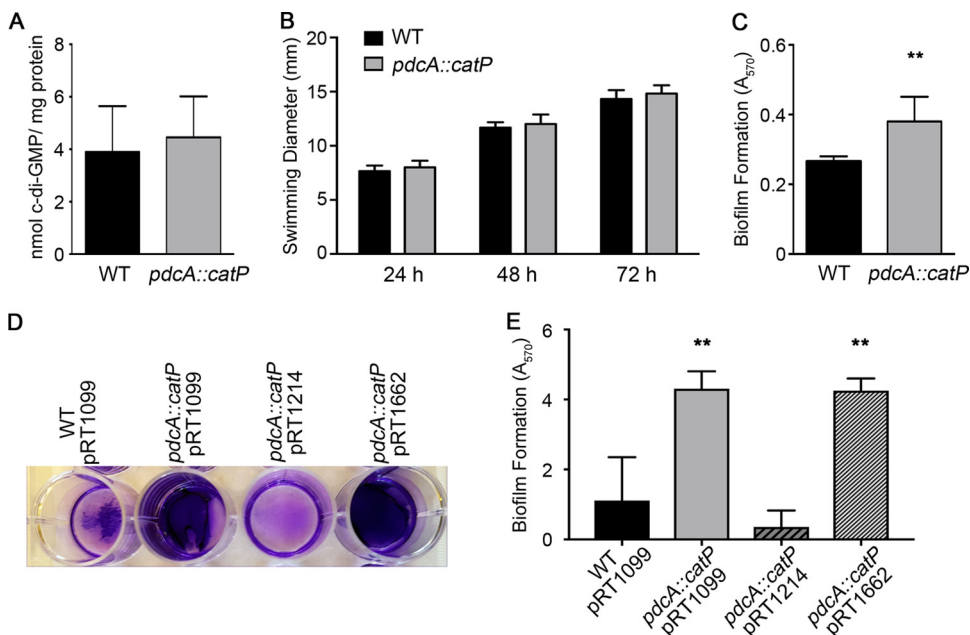


FIG 4 *pdcA* affects biofilm formation but not swimming motility or global *c*-di-GMP levels of *C. difficile*. (A) *c*-di-GMP in the cytoplasm of the 630 WT and *pdcA::catP* mutant *C. difficile* strains was quantified by UPLC-MS and normalized to the total cellular protein level. The mean values and standard deviations of six biologically independent samples are shown. (B) Swimming motility through BHIS–0.3% agar was measured at 24, 48, and 72 h. The mean values and standard deviations of six biologically independent samples are shown. (C) Biofilm formation assayed by crystal violet staining after 24 h of growth. The mean values and standard deviations of five biologically independent samples are shown. **, $P < 0.01$ by unpaired *t* test. (D, E) Complementation analysis of biofilm formation after 24 h of growth. pRT1099 is the vector control, pRT1214 encodes PdcA, and pRT1662 encodes a catalytically inactive form of PdcA. (D) Representative image of crystal violet-stained biofilms. (E) Quantification of biofilm biomass by crystal violet staining. The mean values and standard deviations of three biologically independent samples are shown. **, $P < 0.05$ by one-way analysis of variance and Dunnett’s multiple-comparison test.

c-di-GMP levels under these growth conditions. *C. difficile* motility through brain heart infusion medium with 0.5% yeast extract (BHIS) and 0.3% agar, which is inhibited by high levels of c-di-GMP, was also not altered in the *pdca::catP* mutant (Fig. 4B). In contrast, biofilm formation, which is positively regulated by c-di-GMP (56, 60), was modestly but significantly higher in the *pdca::catP* mutant strain than in the WT (Fig. 4C). The *pdca::catP* mutant expressing *pdca* from a plasmid (pRT1214) under the control of its native promoter produced biofilm comparably to the WT bearing the control vector (pRT1099) (Fig. 4D and E). Expression of an allele of *pdca* encoding an enzymatically inactive PdcA protein in the *pdca::catP* mutant (*pdca* E479A allele, pRT1662) did not restore biofilm formation to WT levels (Fig. 4D and E), indicating that PdcA controls biofilm production via c-di-GMP hydrolysis. Thus, although the *pdca* mutation does not affect global c-di-GMP levels during early stationary phase and does not alter motility through 0.3% agar, increased c-di-GMP as a result of the *pdca* mutation resulted in increased biofilm formation.

***pdca* affects toxin production and cytopathicity.** Production of the *C. difficile* toxins TcdA and TcdB is a stationary-phase phenomenon governed by multiple regulatory factors, including c-di-GMP and CodY (76). Production of TcdR, a sigma factor that positively regulates *tcdA* and *tcdB* expression, is repressed by CodY when GTP and BCAA are abundant in the cytoplasm (27). Expression of *tcdR* is positively regulated by the sigma factor SigD (57, 58). Expression of *sigD* is repressed by elevated c-di-GMP, making c-di-GMP a negative regulator of toxin gene expression (55, 57, 58). To determine whether PdcA activity during stationary phase impacts toxin production, TcdA protein produced by the 630 WT and *pdca::catP* mutant strains, bearing the vector or complementation plasmids indicated, was detected by Western blot analysis. The *pdca::catP* mutant strain with the vector (pRT1099) produced less TcdA than the WT with the vector (Fig. 5A). Expression of *pdca* under the control of its native promoter (pRT1214) partially restored toxin production in the *pdca::catP* mutant strain (Fig. 5A). In contrast, expression of the *pdca* E479A allele (pRT1662) encoding catalytically inactive PdcA did not restore WT levels of toxin production (Fig. 5A). These results support a role for PdcA in the regulation of TcdA production, specifically, the ability to hydrolyze c-di-GMP.

To confirm that diminished TcdA production in the *pdca::catP* mutant strain corresponds to reduced cytopathicity against mammalian cells, we incubated MDCK-LA epithelial cell monolayers overnight with filtered supernatants from stationary-phase cultures of the WT and *pdca::catP* mutant strains. *C. difficile* supernatants, as well as the purified TcdA and TcdB toxins, disrupt the actin cytoskeleton and cause MDCK cell rounding and death (77). We found that a 1:40 dilution of WT supernatant disrupted cell-cell junctions and caused the epithelium to dissociate from the substrate (Fig. 5C). A 1:40 dilution of *pdca::catP* supernatant resulted in some individual cell detachment but left the monolayer largely intact (Fig. 5C). A 1:80 dilution of WT supernatant caused partial cell rounding and dissociation, leaving isolated patches of monolayer intact (Fig. 5C). A 1:80 dilution of *pdca::catP* supernatant had almost no visible effect on monolayer integrity (Fig. 5C). These observations are supported by quantitative evaluation of cell viability after incubation with *C. difficile* supernatants. ATP levels, indicating cell viability, were significantly lower in MDCK-LA cells treated with supernatant from the WT strain than in cells treated with supernatant from the *pdca::catP* mutant strain, indicating reduced cytotoxicity of the *pdca::catP* mutant (Fig. 5B).

To determine whether this reduced cytopathicity was due to reduced toxin production, as opposed to another effect of the *pdca::catP* mutation, we assessed the integrity of the actin cytoskeleton, which is fluorescently labeled in MDCK-LA cells (78). Healthy epithelial cells contain actin stress fibers at the basolateral surface and actin-based microvillus protrusions at the apical surface (Fig. 5D, mock treated) (78). Incubation with WT *C. difficile* lysate resulted in actin depolymerization and perturbed both of these structures (Fig. 5D). Incubation with the same dilution of *pdca::catP* mutant supernatant left these subcellular actin structures largely intact (Fig. 5D). These data suggest that

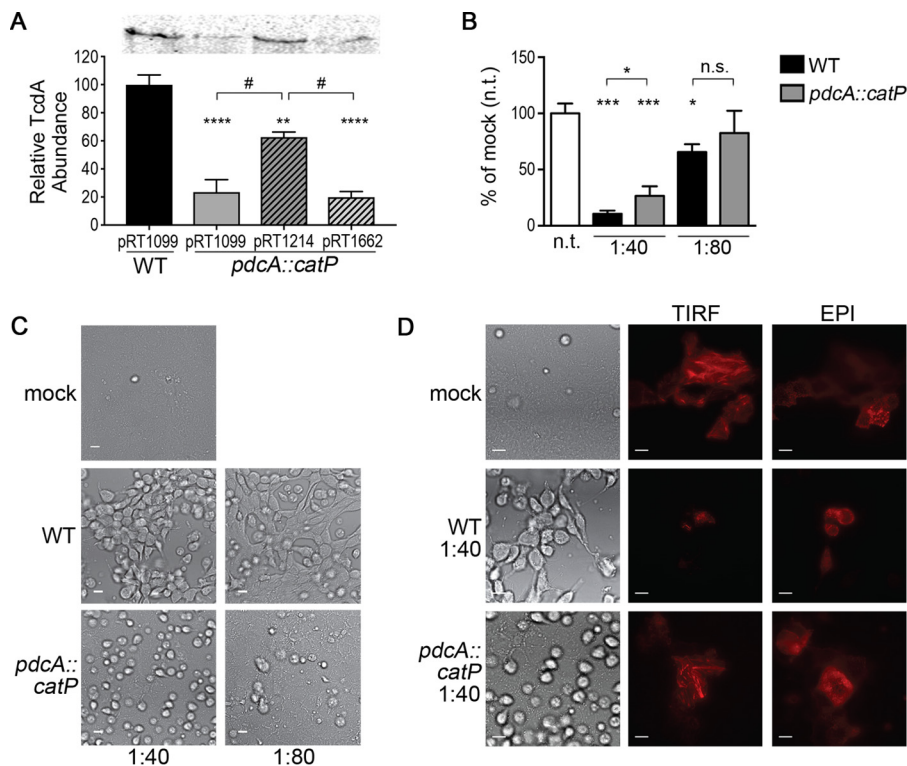


FIG 5 *pdcA* influences *C. difficile* toxin production and cytopathicity. (A) TcdA production by 630/pRT1099 (vector control), *pdcA::catP*/pRT1099 (vector control), *pdcA::catP*/pRT1214 (complementation with *pdcA* WT allele), and *pdcA::catP*/pRT1662 (complementation with *pdcA* E479A mutant allele). Strains were grown for 16 h in TY medium, and lysates were probed for TcdA by Western blot analysis. Samples were normalized by adjustment to the OD of the culture. The data are expressed as a percentage of the 630/pRT1099 value in each respective experiment. The mean values and standard errors from four independent assays are shown. Data were analyzed by one-way analysis of variance and Tukey's multiple-comparison test (**, $P < 0.01$; ****, $P < 0.0001$ compared to 630/pRT1099; #, $P < 0.01$ for the comparisons indicated). A representative Western blot analysis for TcdA is shown at the top. (B) Relative viability of MDCK-LA cells after incubation with supernatants from 630 WT and *pdcA::catP* mutant strain stationary-phase cultures. Data shown are mean values and standard deviations of three biological replicates and were analyzed by two-way analysis of variance and Dunnett's posttest (n.t., not treated; n.s. not significant; *, $P < 0.05$; ***, $P < 0.001$). (C) Cytopathicity of 630 WT and *pdcA::catP* mutant strain supernatants against MDCK-LA cells after 24 h of incubation. Scale bars, 10 μm . (D) Effects of the 630 WT and *pdcA::catP* mutant strains on the actin cytoskeleton (red). TIRF microscopy shows stress fibers at the basolateral cell surface. Epifluorescence shows punctate microvilli at the apical surface. Scale bars, 10 μm .

while the *pdcA::catP* mutation causes a moderate reduction in toxin synthesis, it is a functionally significant difference and is sufficient to render the *pdcA* mutant strain less cytopathic and cytotoxic to mammalian cells.

Growth phase regulation of *pdcA* expression limits the cellular behaviors affected by PdcA. *c*-di-GMP inhibits swimming motility and toxin biosynthesis by repressing the expression of flagellum and toxin genes in *C. difficile* (57, 58), and *c*-di-GMP promotes biofilm formation (56, 60). However, the *pdcA* mutation only had a detectable effect on biofilm formation and toxin production. These results were surprising, because regulation of *tcdA* and *tcdB* by *c*-di-GMP occurs via SigD, which is encoded in the *flgB* operon, whose expression is directly inhibited by *c*-di-GMP (57, 58). We speculated that the directed effect of PdcA on a subset of *c*-di-GMP-regulated processes could be due to restriction of *pdcA* expression to specific conditions and/or to posttranslational control of PdcA function. Given that *pdcA* is a stationary-phase gene (Fig. 2) and the observed biofilm and toxin phenotypes involve stationary-phase bacteria, we hypothesized that temporal regulation of *pdcA* transcription limits PdcA activity to stationary phase. If this is so, we predict that while *pdcA* expression during the motility assay may not be high enough for the *pdcA* mutation to have a measurable effect on bacterial swimming, the *pdcA::catP* mutation will still affect the expression of

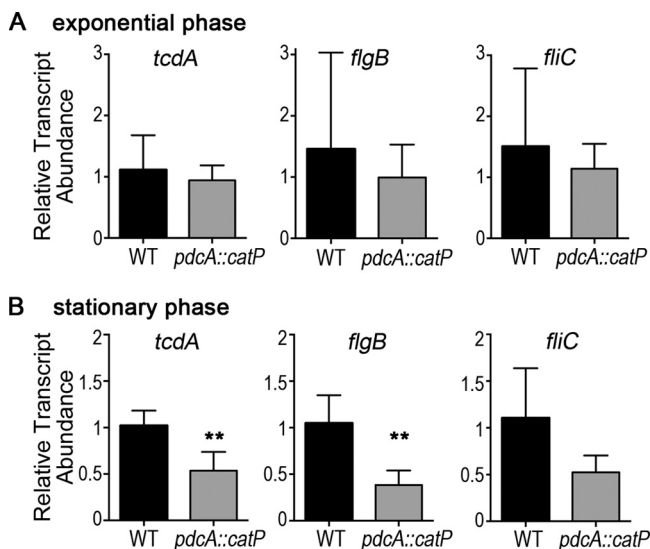


FIG 6 Transcriptional regulation in the *pdcA::catP* mutant. (A) Relative transcript levels of *tcdA*, *flgB*, and *fliC* in WT (black) and *pdcA::catP* mutant (gray) cells during exponential growth. (B) Relative transcript levels during stationary phase. The mean values and standard deviations of five biological replicates are shown. The data were analyzed by unpaired *t* test (**, $P < 0.05$).

both flagellum and toxin genes under stationary-phase conditions. To test this, we compared the expression levels of toxin and flagellar genes in the 630 WT and *pdcA::catP* mutant strains during exponential growth and during stationary phase. We found that transcript levels of *tcdA*, the early flagellar gene *flgB*, and the flagellar filament gene *fliC* were unaffected by the *pdcA::catP* mutation during exponential phase (Fig. 6A). During stationary phase, when *pdcA* is expressed in WT cells, transcript levels of *tcdA* and *flgB* were significantly lower in the *pdcA::catP* mutant strain than in the parental strain (Fig. 6B). The 2-fold reduction observed in toxin gene expression was consistent with the 2-fold reduction in TcdA protein production due to the *pdcA::catP* mutation (Fig. 5A), supporting the conclusion that *pdcA* influences toxin production by regulating gene expression. The *fliC* transcript was also somewhat reduced in the *pdcA::catP* mutant strain during stationary phase, though the differences were not statistically significant ($P = 0.059$) (Fig. 6B). Expression of the WT *pdcA* gene in the *pdcA::catP* mutant partially restored *tcdA* and *fliC* expression, though the differences were not statistically significant (Fig. S3). The expression of the *pdcA* E479A mutant allele had a more modest or no effect (Fig. S3). The challenges of complementing the changes in gene expression in the *pdcA::catP* mutant are likely due to the small effects of the *pdcA* mutation on transcript levels. Thus, the *pdcA* mutation affects the regulation of flagellar genes in addition to the toxin genes under nutrient-limited conditions in which *pdcA* is expressed, suggesting that genes expressed during stationary phase have limited effects on motility through soft agar.

DISCUSSION

In this work, we expanded our prior understanding of c-di-GMP regulation in *C. difficile* by characterizing the regulation and function of PdcA, 1 of 19 known or putative c-di-GMP PDEs in *C. difficile* strain 630. We had previously reported that overexpression of the PdcA-EAL domain had no discernible effect on *C. difficile* physiology or behavior and speculated that cytoplasmic c-di-GMP levels were low enough under the conditions studied to preclude a significant reduction upon ectopic PDE overproduction (55). Here, we show that the activity of the PdcA regulatory domains and growth phase regulation of *pdcA* expression determine PdcA-dependent phenotypes.

Disruption of *pdcA* significantly impacts biofilm formation and toxin biosynthesis. Disruption of *pdcA* does not affect flagellar motility through soft agar, although the

pdca mutation does affect flagellar gene expression during stationary phase. We speculate that this distinction is due to the conditions of the motility assay. As flagellar motility assays involve bacterial cells continuously expanding into conditions of low cell density and fresh, nutrient-rich medium, the effects of stationary-phase genes may not be readily apparent. In contrast, *C. difficile* toxins are produced in stationary-phase cultures *in vitro* (27) and biofilms are likely to contain stationary-phase bacteria, making it possible to detect the effects of a *pdca* mutation. Thus, CodY inhibition of *pdca* transcription during exponential growth results in temporal regulation that directs PdcA activity toward the c-di-GMP-regulated processes that occur during stationary phase.

In vitro assays of PDE activity of PdcA and mutant derivatives indicate that the PAS domain is required for full activity and suggest that GTP binding to the GGDEF domain stimulates the enzymatic activity of the EAL domain. These results are supported by *in vivo* analyses. While ectopic expression of WT, full-length *pdca* significantly increased swimming motility, expression of the mutant derivatives did not, although they were catalytically active. Together, these data indicate that PdcA activity is regulated at the protein level. The ability of degenerate GGDEF domains to regulate a tandem EAL domain in response to GTP has been demonstrated (68, 79), and it remains possible that the PdcA PAS domain provides another as-yet-uncharacterized means of post-translational regulation. Of the 19 *C. difficile* EAL family c-di-GMP PDEs, 18 contain degenerate GGDEF domains (80), suggesting that c-di-GMP turnover in *C. difficile* may be generally linked to GTP availability (65–67). As c-di-GMP synthesis utilizes GTP as a substrate, linking c-di-GMP hydrolysis to GTP availability may limit c-di-GMP turnover under nutrient-limiting growth conditions when intracellular GTP availability is limited (33, 34, 65, 81–83).

A DNA region encompassing the 5' end of the *pdca* ORF and putative promoter was identified as a target of CodY binding (27). That study did not identify a consensus CodY binding site in the *pdca* promoter region. However, we demonstrate that CodY binds directly to the *pdca* promoter region *in vitro*. We note that Dineen et al. allowed up to three mismatches from the CodY consensus, whereas the putative CodY binding site upstream of the *pdca* coding sequence contains four bases that deviate from the consensus (Fig. S2). Lower concentrations of CodY bound to and shifted the DNA fragment containing the *ilvC* promoter, suggesting higher affinity of CodY for the *ilvC* promoter than for the *pdca* promoter, consistent with the greater transcriptional repression by CodY observed for *ilvC*.

Regulation of *pdca* transcription by CodY further links PdcA activity to cytoplasmic GTP. Interestingly, CodY and PdcA appear to have dramatically different affinities for GTP *in vitro*. Purified *C. difficile* CodY is activated *in vitro* only by very large (10,000-fold) molar excesses of GTP (30, 84), while purified PdcA is activated by an equimolar amount of GTP, suggesting that PdcA activity may be stimulated by GTP concentrations too low to activate CodY. This suggests that fluctuations in cytoplasmic GTP levels can impact the transcription of the *pdca* gene, as well as modulate the activity of previously expressed PdcA protein (Fig. 7). At limiting GTP concentrations, the enzymatic activity of PdcA is likely to be low, but deactivation of CodY would allow *pdca* transcription to increase the overall level of PdcA in the cell cytoplasm. At the other extreme, very high GTP levels would inhibit *pdca* transcription via CodY, but the activity of existing PdcA molecules would be maximal. In both *B. subtilis* and *S. aureus*, CodY functions as a “dimmer” rather than a binary on-off switch, repressing certain genes differentially in response to moderate or severe levels of nutrient limitation (85, 86). It is likely that in *C. difficile* many circumstances *in vivo* could feature intermediate cytoplasmic GTP levels low enough to allow some *pdca* expression but high enough to permit stimulation of PdcA enzymatic activity (Fig. 7). As intracellular GTP concentrations in bacteria are highly dynamic and responsive to the addition of nutrients to the growth medium, with transient 70 to 80% decreases in the cytoplasmic GTP concentration and concomitant rises in ppGpp occurring upon stationary phase onset or during starvation (32–34,

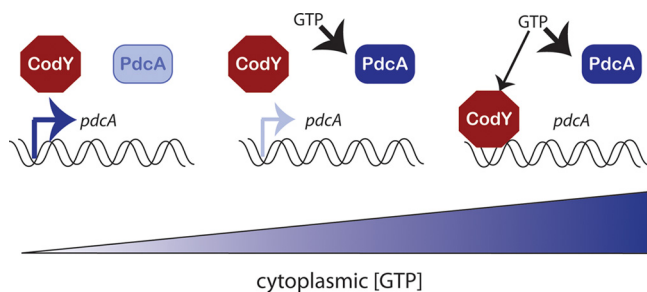


FIG 7 GTP levels inversely regulate the production and activity of PdcA enzymes. At very low cytoplasmic GTP levels, the activity level of existing PdcA proteins will be low, but CodY will be deactivated to permit additional *pdca* transcription. At intermediate concentrations, both *pdca* transcription and PdcA activity will be responsive to GTP fluctuations. At high GTP levels, *pdca* transcription will be inhibited but existing PdcA will be very active.

81–84, 87), the net PdcA activity in the cell may be highly responsive to intracellular GTP availability and extracellular nutrient availability.

c-di-GMP signaling is affected by nutrient limitation in other bacterial species. For example, multiple *Pseudomonas* species have been shown to increase the expression of PDE genes in response to nutrient starvation, although these genes have been implicated in biofilm dispersal rather than biofilm formation or motility (88, 89). Similarly, a bifunctional DGC-PDE protein affects the long-term survival of *Mycobacterium smegmatis* under nutrient-limiting conditions (90). Nutrient limitation is a clinically relevant stress for intestinal pathogens: the healthy mammalian large intestine is not rich in usable nutrient sources for *C. difficile*, as mono- and disaccharides and amino acids are largely absorbed by the host in the small intestine (91, 92). The recent discovery that a “nutrient bloom” in response to antibiotic disruption of the gut microbiome increases susceptibility to *C. difficile* infection suggests that nutrient availability is a major barrier to *C. difficile* survival in a healthy host (93). It is worth noting that *pdca* (CD630_15150) expression is also increased by heat shock, another clinically relevant stress (94), raising the possibility that this PDE controls a more general stress response in *C. difficile*.

This is the first report linking any c-di-GMP-regulated phenotypes in *C. difficile* to the activity of a specific c-di-GMP metabolism protein, underscoring the importance of analyzing individual PDE and DGC enzymes. Future studies to more precisely identify the extracellular nutrient signals that affect PdcA activity will help define the environmental conditions that influence c-di-GMP signaling in *C. difficile*. Further work to determine the chemical signals that modulate intracellular c-di-GMP in *C. difficile* is vital, given the role of this second messenger in the control of processes central to pathogenesis.

MATERIALS AND METHODS

Bacterial strains and growth conditions. The bacterial strains and plasmids used in this study are listed in Table S1. *C. difficile* 630 and derivative strains were routinely grown in BHIS, supplemented as specified, in an anaerobic chamber with an atmosphere of 85% N₂, 5% CO₂, and 10% H₂. Medium for growth of strains containing pMC123 derivative plasmids was supplemented with 10 μg/ml thiamphenicol (BHIS-Tm). Medium for growth of strains containing the integrated pSD21 *codY* insertional mutation was supplemented with 2 μg/ml erythromycin (BHIS-Erm). Medium for growth of strains containing pRT1099, pRT1214, or pRT1662 was supplemented with 500 μg/ml spectinomycin unless indicated otherwise. *Escherichia coli* strains were propagated in Luria-Bertani (LB) medium or on LB agar plates containing 50 μg/ml ampicillin, 10 μg/ml chloramphenicol, and/or 50 μg/ml spectinomycin, as needed, at 37°C under aerobic conditions.

Plasmid and strain construction. All restriction enzymes and DNA polymerase (Phusion) were purchased from New England BioLabs. The sequences of the oligonucleotides used in this study are listed in Table S2.

The creation of pMMBneo::*pdca* and pMMBneo::*pdca*-EAL has previously been described (55). Purified pMMBneo::*pdca* (55) was used as the PCR template to generate *E. coli* expression constructs. A mutant allele of *pdca* (CD630_1515) in which the GGDEF motif, sequence DGDEM, is mutated to alanines was generated by splicing by overhang extension (SOE) PCR. Primers *pdca*F and *pdca*AgaR were used to amplify the upstream fragment, and primers *pdca*AgaF and *pdca*AR were used to amplify the downstream fragment, and they were subsequently spliced together. A PdcA truncation lacking the N-terminal PAS

domain (residues 1 to 251) was amplified from pMMBneo::*pdca* with primers *pdca*AdpF and *pdca*AR. The resulting fragments were digested with KpnI and PstI and ligated to similarly digested pMMBneo (95). Kanamycin-resistant transformants of *E. coli* DH5 α were screened for the desired plasmids by PCR with gene-specific primers and plasmid-specific primers 67EHF and 67EHR. The plasmids were introduced by electroporation into *E. coli* BL21 for gene expression and protein purification.

For gene expression in *C. difficile*, pPdcA (55) was the PCR template for generating a GGDEF point mutant and a Δ PAS truncation with the primers listed above. The resulting fragments were digested with KpnI and PstI and ligated to similarly digested pMC-Pcpr. Chloramphenicol-resistant transformants of *E. coli* DH5 α were screened for the desired plasmids by PCR with primers pUCmScF and m13R. These plasmids were transformed by electroporation into strain HB101(pRK24) to allow conjugation with *C. difficile*. The HB101(pRK24) plasmid donor strains were mated with *C. difficile* strain 630 as previously described (55). Transconjugants were selected on BHIS-Tm supplemented with 100 μ g/ml kanamycin and screened by PCR with pUCmScF and m13R to confirm the presence of a plasmid with an insert of the correct size and with primers *tcdBF* and *tcdBR* to confirm the isolation of *C. difficile*. At least two isolates were obtained for each conjugation. The generation of pPdcA and pPdcA-EAL and their introduction into *C. difficile* were previously described (55).

The *pdca::catP* mutant was created by double homologous recombination essentially as previously described, with some modifications (75). Allelic-exchange vector pMC234 was created by the stepwise addition of two DNA fragments to pUC19 (96). A 390-bp *oriT* fragment was PCR amplified from pJIR1456 (97) with primers oMC15 and oMC16, digested with EcoO1091/AatII, and ligated into pUC19 to give plasmid pMC95 (98). A 1,043-bp fragment containing the *C. perfringens catP* gene was then amplified from pJIR1456 (97) with primers oMC2 and oMC143, digested with BamHI, and ligated into pMC95 to yield plasmid pMC234. The 2,000-bp regions upstream and downstream of the *pdca* ORF were amplified with primers *pdca*F1 and *pdca*R1 or *pdca*F2 and *pdca*R2, respectively. The 5' flanking region was digested with EcoRI and KpnI, and the 3' flanking region was digested with Sall and PstI. Fragments were sequentially ligated into pMC234, flanking the *catP* gene, to create pMC234::*pdca::catP*, which was transformed by electroporation into HB101(pRK24) for conjugation with *C. difficile* 630. Isolates with a single-crossover integration of pMC234::*pdca::catP* were selected on BHIS-Tm plates supplemented with 100 μ g/ml kanamycin to select against HB101(pRK24). Thiamphenicol-resistant single-crossover isolates were confirmed by PCR with primers within the sequences flanking the *pdca* ORF, which yield a 2.1-kb product when amplifying *pdca* from the chromosome and a 1.1-kb product when amplifying *catP* from the integrated plasmid. Primers PdcAF and PdcAR, which amplify the *pdca* ORF but not the flanking sequences, were used to specifically detect *pdca*, and oMC143 and oMC2 were used to specifically detect *catP*. Additional screening was performed with the flanking primer pair *pdca*AbamHI and *pdca*ApstI or *pdca*AbamHI and PdcAR0, which will amplify the WT *pdca* ORF on the chromosome but yield no product from the integrated vector. Isolates were passaged once in BHIS-Tm broth and subsequently in BHIS with no antibiotic. Each passage was plated on BHIS agar, and individual colonies were screened by PCR with multiple pairs of primers. After eight passages, we obtained a strain in which the *pdca* gene (2,094 bp) was replaced with the *catP* gene (1,043 bp). The loss of integrated pMC234::*pdca::catP* was confirmed by PCR screening for the *bla* gene on the vector with primers *blaF* and *blaR*.

To create vectors encoding spectinomycin resistance, the *Enterococcus faecalis aad9* gene was amplified from pBTS (gift from A. R. Richardson) (99) with primers *aad9F_EcoRV* and *aad9R_EcoRV* and digested with EcoRV. pMC123 was digested with SapI and PciI to remove the *catP* cassette and then treated with Klenow fragment to blunt the ends. The *aad9* gene was ligated into pMC123 lacking *catP*, generating pRT1099. *pdca* and the 521 bp upstream of the translational start site were amplified from *C. difficile* genomic DNA with primers *pdca*PromF and *pdca*PromR and ligated into pRT1099 at the SphI and BamHI restriction sites to create pRT1214. A *pdca* E479A mutant allele with an alanine substitution of glutamic acid in the EAL motif was generated by SOE PCR with primers *pdca*Aeaf and *pdca*Aear. Primers *pdca*PromF and *pdca*Aear were used to amplify the upstream fragment of *C. difficile* 630 genomic DNA, and primers *pdca*Aeaf and *pdca*PromR were used to amplify the downstream fragment. The fragments were spliced together and cloned into pRT1099 at the SphI and BamHI restriction sites, yielding pRT1662. The plasmids were confirmed by PCR and sequencing of the cloned fragment and then introduced into *C. difficile* by conjugation via HB101(pRK24).

RNA isolation and qRT-PCR. RNA was isolated as described previously from *C. difficile* cultures grown in BHIS with the appropriate antibiotics to exponential or early stationary phase as previously indicated (55). Exponential-phase samples were collected at an optical density at 600 nm (OD_{600}) of 0.4 to 0.6, and stationary-phase samples were collected 1 to 2 h after logarithmic growth ended. After DNase treatment (Ambion), cDNA samples were prepared from 500 ng of RNA with random hexamers and the Tetro cDNA synthesis kit (Bioline). Real-time PCR was done with 4 ng of template cDNA with the SensiMix SYBR and fluorescein kit (Bioline). Primers (Table S2) were designed with the PrimerQuest tool from IDT DNA Technologies, and forward and reverse primers were named in accordance with the pattern gene-qF and gene-qR, respectively. At least three independent samples were analyzed. The *rpoC* transcript was used as the reference gene (55). Controls with no reverse transcriptase were included for all templates and all primer sets. The data were analyzed by the $2^{-\Delta\Delta CT}$ method, with normalization to *rpoC* and the stated reference condition or strain (55).

Protein purification. BL21 expression strains were grown at 37°C to an OD_{600} of 0.1 to 0.15, at which point the cultures were shifted to 25°C and expression was induced with 1 mM isopropyl- β -D-thiogalactopyranoside (IPTG) for 16 h. Cells were collected by centrifugation and lysed by sonication in His6 buffer (10 mM Tris-HCl [pH 7.8], 300 mM NaCl, 50 mM NaH₂PO₄, 10% glycerol) supplemented with 1 mM phenylmethylsulfonyl fluoride (PMSF) and 1 mg/ml lysozyme (55). Lysates were clarified by

centrifugation at $12,000 \times g$ for 30 min at 4°C, and the soluble fractions were incubated with HisPur Ni-nitrilotriacetic acid (NTA) resin (Thermo Scientific) for 2 h at 4°C. Samples were centrifuged at $700 \times g$ for 2 min at 4°C, and then the resin was suspended in His6 buffer, rocked for 15 min at 4°C, and centrifuged at $700 \times g$ for 2 min at 4°C. This washing protocol was repeated twice with His6 buffer containing 100 mM imidazole. Proteins were eluted in His6 buffer with 250 mM imidazole. Purified proteins were confirmed by SDS-PAGE and staining with Coomassie brilliant blue (55). Protein concentrations were measured by UV spectroscopy by using ϵ_{280} values calculated from ExPASy ProtParam (100). Purified proteins were stored at 4°C and used for enzymatic assays within 5 days of purification.

Histidine-tagged CodY was purified from *E. coli* BL21 bearing pEAV1 (30). The strain was grown at 37°C to an OD₆₀₀ of 0.4 to 0.5, and then IPTG was added to a final concentration of 1 mM. After an additional 5 h of growth at 37°C, cells were collected by centrifugation. The pellet was suspended in BugBuster Lysis Solution (EMD Millipore), and cells were lysed in accordance with the manufacturer's protocol. The soluble fraction was collected by centrifugation and incubated with HisPur Ni-NTA resin for 2 h at 4°C. The resin was washed with CodY buffer (20 mM Tris [pH 8], 125 mM KCl, 50 mM NaH₂PO₄, 10% glycerol, 1 mM PMSF) containing 50 mM imidazole. CodY was eluted with CodY buffer containing 200 mM imidazole. Amicon Ultrafree columns with a 3,000-Da molecular mass cutoff (EMD Millipore) were used for buffer exchange and protein concentration into CodY buffer. Protein concentration was determined with the Pierce BCE Protein Assay kit (Thermo Scientific). Glycerol was added to a final concentration of 20%, and the protein was stored at -20°C.

In vitro enzymatic assays. Purified PdcA, PdcA(GA), PdcA-ΔPAS, and PdcA-EAL were assayed for PDE activity as previously described (55). The radiolabeled c-di-GMP substrate was synthesized by using the characterized *C. difficile* DGC DccA and purified as described previously (101, 102). The reaction was initiated by the addition of radiolabeled substrate, and 1-μl aliquots were taken for analysis at 6, 30, 60, and 120 s. Reaction mixtures lacking enzyme were used as negative controls. Where specified, 0, 1, 20, or 100 μM GTP was added to the reaction mixtures. Aliquots were analyzed by thin-layer chromatography as described previously (102). All reaction mixtures were prepared in triplicate. Enzymatic activity was recorded as the percentage of ³²P-labeled c-di-GMP cleaved over time.

EMSA. Binding of CodY to the *pdcA* promoter, as well as an *ilvC* promoter positive control, was assessed by EMSA essentially as described previously (30). A region encompassing the first 145 nucleotides of the *pdcA* coding sequence and 261 upstream bases was amplified from *C. difficile* 630 chromosomal DNA by PCR with *pdcA*emsaF and *pdcA*emsaR. The 423-bp *ilvC* promoter region was amplified with OSD107 and OSD108 (27). As a negative control, a 133-bp fragment of the *gfpA* gene was amplified from *V. cholerae* C6706 chromosomal DNA with primers *gfpA*qF and *gfpA*qR (103). Binding reactions between CodY and putative target DNA took place in a mixture of 20 mM Tris (pH 8); 50 mM sodium glutamate; 10 mM MgCl₂; 5 mM EDTA; 0.1% Tween 20; 5% glycerol; 2 mM GTP; and 100 mM each leucine, isoleucine, and valine (30). Binding reaction mixtures contained serially diluted CodY, 50 ng of *V. cholerae gfpA* DNA, and 70 ng of either *ilvC* promoter DNA or *pdcA* promoter DNA and were incubated at room temperature for 30 min. Samples were separated by electrophoresis in 10% Mini-PROTEAN TGX precast gels (Bio-Rad) in a running buffer consisting of 25 mM Tris base, 192 mM glycine, and 10 mM isoleucine-leucine-valine. Gels were stained for 1 h with GelRed (Biotium) and imaged under UV light.

c-di-GMP quantification by UPLC-MS. Nucleotides were extracted from *C. difficile* and quantified as previously described (60). Briefly, individual colonies of the 630 WT and *pdcA::catP* mutant strains were grown anaerobically at 37°C for 7 h. These starter cultures were diluted 1:100 in 50 ml of BHIS medium and grown anaerobically at 37°C for 10 h to an OD₆₀₀ of 1.6 to 1.8. Nucleotides were isolated from the supernatant through methanol-acetonitrile extraction as previously described (60). The total protein content of the insoluble fraction of each sample was quantified by the colorimetric BCA assay kit (Thermo Scientific). Nucleotide samples were dried overnight with a vacuum concentrator at room temperature and suspended in 100 μl of distilled H₂O/200 μl of extracted nucleotide. Samples were stored at -80°C until use. Aliquots (10 μl) were injected into a TSQ Quantum Ultra triple-quadrupole mass analyzer (Thermo Scientific, Waltham, MA). The analytes were separated on a Waters HSS T3 UPLC column (2.1 by 100 mm, 1.8 μm) by gradient elution from 99.9% solvent A (10 mM ammonium formate in water) to 40% solvent B (10 mM ammonium formate in methanol) for 2 min, followed by column flushing at 90% solvent B for 2.5 min and column re-equilibration for 3.5 min. The column effluent was diverted to waste for the first 2 min. The mass spectrometer parameters were as follows: positive-ion electrospray mode; spray voltage, 3.5 kV; vaporizer temperature, 250°C; sheath gas, 35 arbitrary units; auxiliary gas, 30 arbitrary units; capillary temperature, 285°C; collision gas pressure, 1.5 mtorr (0.19 Pa). c-di-GMP was detected by monitoring precursor ion-to-fragment ion transitions (*m/z* 691 to >152 [collision energy, 35] and *m/z* 691 to >540 [collision energy, 21]) and quantified by using a calibration curve of known concentrations of pure c-di-GMP (Biolog Life Science Institute, Bremen, Germany) ranging from 0.1 to 1,000 nM. Cytoplasmic c-di-GMP concentrations were normalized to the total protein content of the samples. Four independent samples were analyzed for each strain.

Motility assays. Motility experiments were performed as previously described (55). Briefly, individual colonies were inoculated with sterile toothpicks into 0.3% agar plates containing BHIS or BHIS-Tm with 0 or 5 μg/ml nisin. The plates were incubated at 37°C in an anaerobic chamber for 72 h. The diameters of motility growth were measured every 24 h for three independent experiments.

Detection of TcdA by Western blot analysis. Overnight cultures were diluted 1:100 in tryptone-yeast (TY) medium with 250 μg/ml spectinomycin (104). After 16 h of growth under anaerobic conditions at 37°C, bacteria were collected from 3 ml of culture by centrifugation and suspended in SDS-PAGE loading buffer. Samples were normalized to the ODs of the cultures for loading onto 4 to 15% TGX polyacrylamide gradient gels (Bio-Rad). After electrophoresis, the samples were transferred to nitrocel-

lulose membranes. Blots were probed with a mouse anti-TcdA antibody (Novus Biologicals) and an IR800-conjugated goat anti-mouse secondary antibody (Thermo Fisher) and visualized on an Odyssey Imager (Li-COR Biotechnology). The anti-TcdA signal was quantified with Image Studio (Li-COR Biotechnology). Four independent experiments were done, and the data are expressed as percentages of the strain 630/pRT1099 (WT with vector) value in that experiment.

Biofilm assays. Untreated polystyrene 24-well culture plates (Corning) were kept in an anaerobic chamber for a minimum of 72 h prior to use. Overnight cultures were diluted 1:50 in 1 ml of BHIS supplemented with 1% glucose and 50 mM sodium phosphate buffer (pH 7.5). For experiments with *C. difficile* bearing pRT1099 and derivatives, 250 μ g/ml spectinomycin was added to the medium. After incubation at 37°C for 24 h under anaerobic conditions, the culture supernatant was removed and the adherent biomass was washed once with phosphate-buffered saline (PBS) and stained for 30 min with 0.1% (wt/vol) crystal violet in water. Excess crystal violet was removed, and the wells were washed twice with PBS. The bound crystal violet was solubilized with 95% ethanol. The absorbance at 570 nm was measured with a Synergy HT microplate reader (BioTek). Experiments were done at least three times.

Analysis of cytopathic effects on target cells. The WT and *pdca::catP* mutant *C. difficile* strains were grown in BHIS medium supplemented with 50 mM sodium phosphate buffer (pH 7.5) for 24 h. Cultures were centrifuged for 5 min at 2,000 \times *g*, and supernatants were filtered through 0.45- μ m sterile nylon filters (Fisher). MDCK cells stably expressing LifeAct-tagRFP-T (ibidi USA) (78) were generated as described in reference 105. Briefly, type II MDCK cells (clone T23; Invitrogen) were cotransfected with pLL5/LifeAct-tagRFP-T and pTK-Hyg. The transfected cells were cultured with selection medium containing 250 μ g/ml hygromycin B (Roche). Clones were selected by red fluorescent protein (RFP) fluorescence and confirmed by Western blot analysis for tagRFP protein and are termed MDCK-LA cells here. For cytopathicity assays, MDCK-LA cells were seeded at high density and grown for 2 days after confluence was reached in Dulbecco's modified Eagle medium supplemented with 10% fetal bovine serum (F2442; Sigma) in 24-well tissue culture plates (3524; Costar) at 37°C and 5% CO₂. Samples were then incubated with the dilutions of bacterial supernatant indicated at 37°C and 5% CO₂ for 24 h. For quantitative measurements of cell viability, ATP content was measured with the CellTiter-Glo Luminescent Cell Viability assay (Promega).

MDCK cells were imaged with a Nikon TiE microscope equipped with a Hamamatsu Orca-Flash 4.0 camera. Cells in plates were imaged with Nikon 10 \times /numerical aperture (NA) 0.25 (Plan, Ph1 DL) and 20 \times /NA 0.75 (Plan Apo, Ph2 DM) objectives in conjunction with phase-contrast and differential interference contrast optical components, as indicated. For visualization of the actin cytoskeleton, cells were grown in 35-mm glass bottom dishes (P35G-1.5-20-C; MatTek) and visualized with the same microscope with a laser with a 568-nm wavelength for total internal reflection fluorescence (TIRF) and epifluorescence through a 60 \times /NA 1.45 (Plan Apo TIRF) objective. All imaging data were collected with Nikon Elements. Image analysis was performed with Nikon Elements and ImageJ.

SUPPLEMENTAL MATERIAL

Supplemental material for this article may be found at <https://doi.org/10.1128/IAI.00347-17>.

SUPPLEMENTAL FILE 1, PDF file, 0.6 MB.

ACKNOWLEDGMENTS

We thank Abraham Sonenshein for the JIR8094/pSD21 strain and for pEAV1.

This research was supported by NIH grants U54-AI057157 and R01-AI107029 to R.T., R01-DC003299 to R.E.C., and K01-DK087763 to S.M.M. E.B.P. was supported by T32-DK007737 to the Center for Gastrointestinal Biology and Disease, and D.S.C. was supported by T32-CA009156 to the Lineberger Comprehensive Cancer Center. UPLC-MS was performed at the University of North Carolina Environmental Sciences and Engineering Biomarker Mass Spectrometry Core Facility, which is supported in part by a grant from the National Institute of Environmental Health Sciences (P30ES010126). The contents of this report are solely the responsibility of the authors and do not necessarily represent the official views of the funding bodies.

REFERENCES

1. Miller M. 2010. Fidaxomicin (OPT-80) for the treatment of *Clostridium difficile* infection. *Expert Opin Pharmacother* 11:1569–1578. <https://doi.org/10.1517/14656566.2010.485614>.
2. Buffe CG, Bucci V, Stein RR, McKenney PT, Ling L, Gouborne A, No D, Liu H, Kinnebrew M, Viale A, Littmann E, van den Brink MR, Jenq RR, Taur Y, Sander C, Cross JR, Toussaint NC, Xavier JB, Pamer EG. 2015. Precision microbiome reconstitution restores bile acid mediated resistance to *Clostridium difficile*. *Nature* 517:205–208. <https://doi.org/10.1038/nature13828>.
3. Britton RA, Young VB. 2014. Role of the intestinal microbiota in resistance to colonization by *Clostridium difficile*. *Gastroenterology* 146:1547–1553. <https://doi.org/10.1053/j.gastro.2014.01.059>.
4. de La Cochetière M-F, Montassier E, Hardouin J-B, Carton T, Vacon F, Durand T, Lalande V, Petit J, Potel G, Beaugerie L. 2010. Human intestinal microbiota gene risk factors for antibiotic-associated diarrhea: perspectives for prevention. *Microb Ecol* 59:830–837. <https://doi.org/10.1007/s00248-010-9637-2>.
5. Manges AR, Labbe A, Loo VG, Atherton JK, Behr MA, Masson L, Tellis PA, Brousseau R. 2010. Comparative metagenomic study of alterations to the intestinal microbiota and risk of nosocomial *Clostridium difficile*.

- associated disease. *J Infect Dis* 202:1877–1884. <https://doi.org/10.1086/657319>.
6. Ng KM, Ferreyra JA, Higginbottom SK, Lynch JB, Kashyap PC, Gopinath S, Naidu N, Choudhury B, Weimer BC, Monack DM, Sonnenburg JL. 2013. Microbiota-liberated host sugars facilitate post-antibiotic expansion of enteric pathogens. *Nature* 502:96–99. <https://doi.org/10.1038/nature12503>.
 7. Theriot CM, Koenigsnecht MJ, Carlson PE, Jr, Hatton GE, Nelson AM, Li B, Huffnagle GB, Li J, Young VB. 2014. Antibiotic-induced shifts in the mouse gut microbiome and metabolome increase susceptibility to *Clostridium difficile* infection. *Nat Commun* 5:3114. <https://doi.org/10.1038/ncomms4114>.
 8. Sambol SP, Tang JK, Merrigan MM, Johnson S, Gerding DN. 2001. Infection of hamsters with epidemiologically important strains of *Clostridium difficile*. *J Infect Dis* 183:1760–1766. <https://doi.org/10.1086/320736>.
 9. Rodriguez-Palacios A, Lejeune JT. 2011. Moist-heat resistance, spore aging, and superdormancy in *Clostridium difficile*. *Appl Environ Microbiol* 77:3085–3091. <https://doi.org/10.1128/AEM.01589-10>.
 10. Vohra P, Poxton IR. 2011. Comparison of toxin and spore production in clinically relevant strains of *Clostridium difficile*. *Microbiology* 157:1343–1353. <https://doi.org/10.1099/mic.0.046243-0>.
 11. Sorg JA, Sonenshein AL. 2008. Bile salts and glycine as cogerminants for *Clostridium difficile* spores. *J Bacteriol* 190:2505–2512. <https://doi.org/10.1128/JB.01765-07>.
 12. Howerton A, Ramirez N, Abel-Santos E. 2011. Mapping interactions between germinants and *Clostridium difficile* spores. *J Bacteriol* 193:274–282. <https://doi.org/10.1128/JB.00980-10>.
 13. Di Bella S, Ascenzi P, Siarakas S, Petrosillo N, di Masi A. 2016. *Clostridium difficile* toxins A and B: insights into pathogenic properties and extraintestinal effects. *Toxins (Basel)* 8:E134. <https://doi.org/10.3390/toxins8050134>.
 14. Voth DE, Ballard JD. 2005. *Clostridium difficile* toxins: mechanism of action and role in disease. *Clin Microbiol Rev* 18:247–263. <https://doi.org/10.1128/CMR.18.2.247-263.2005>.
 15. Just I, Fritz G, Aktories K, Giry M, Popoff MR, Boquet P, Hegenbarth S, von Eichel-Streiber C. 1994. *Clostridium difficile* toxin B acts on the GTP-binding protein Rho. *J Biol Chem* 269:10706–10712.
 16. Just I, Selzer J, von Eichel-Streiber C, Aktories K. 1995. The low molecular mass GTP-binding protein Rho is affected by toxin A from *Clostridium difficile*. *J Clin Invest* 95:1026–1031. <https://doi.org/10.1172/JCI117747>.
 17. Dillon ST, Rubin EJ, Yakubovich M, Pothoulakis C, LaMont JT, Feig LA, Gilbert RJ. 1995. Involvement of Ras-related Rho proteins in the mechanisms of action of *Clostridium difficile* toxin A and toxin B. *Infect Immun* 63:1421–1426.
 18. Burridge K, Wennerberg K. 2004. Rho and Rac take center stage. *Cell* 116:167–179. [https://doi.org/10.1016/S0092-8674\(04\)00003-0](https://doi.org/10.1016/S0092-8674(04)00003-0).
 19. Ottlinger ME, Lin S. 1988. *Clostridium difficile* toxin B induces reorganization of actin, vinculin, and talin in cultured cells. *Exp Cell Res* 174:215–229. [https://doi.org/10.1016/0014-4827\(88\)90156-5](https://doi.org/10.1016/0014-4827(88)90156-5).
 20. Ng J, Hirota SA, Gross O, Li Y, Ulke-Lemea A, Potentier MS, Schenck LP, Vilaysane A, Seamone ME, Feng H, Armstrong GD, Tschopp J, Macdonald JA, Muruve DA, Beck PL. 2010. *Clostridium difficile* toxin-induced inflammation and intestinal injury are mediated by the inflammasome. *Gastroenterology* 139:542–552, 552 e541–543. <https://doi.org/10.1053/j.gastro.2010.04.005>.
 21. Chen S, Sun C, Wang H, Wang J. 2015. The role of Rho GTPases in toxicity of *Clostridium difficile* toxins. *Toxins (Basel)* 7:5254–5267. <https://doi.org/10.3390/toxins7124874>.
 22. Kuipers EJ, Surawicz CM. 2008. *Clostridium difficile* infection. *Lancet* 371:1486–1488. [https://doi.org/10.1016/S0140-6736\(08\)60635-2](https://doi.org/10.1016/S0140-6736(08)60635-2).
 23. McCollum DL, Rodriguez JM. 2012. Detection, treatment, and prevention of *Clostridium difficile* infection. *Clin Gastroenterol Hepatol* 10:581–592. <https://doi.org/10.1016/j.cgh.2012.03.008>.
 24. Deakin LJ, Clare S, Fagan RP, Dawson LF, Pickard DJ, West MR, Wren BW, Fairweather NF, Dougan G, Lawley TD. 2012. The *Clostridium difficile* *spo0A* gene is a persistence and transmission factor. *Infect Immun* 80:2704–2711. <https://doi.org/10.1128/IAI.00147-12>.
 25. Edwards AN, Nawrocki KL, McBride SM. 2014. Conserved oligopeptide permeases modulate sporulation initiation in *Clostridium difficile*. *Infect Immun* 82:4276–4291. <https://doi.org/10.1128/IAI.02323-14>.
 26. Nawrocki KL, Edwards AN, Daou N, Bouillaut L, McBride SM. 2016. CodY-dependent regulation of sporulation in *Clostridium difficile*. *J Bacteriol* 198:2113–2130. <https://doi.org/10.1128/Jb.00220-16>.
 27. Dineen SS, McBride SM, Sonenshein AL. 2010. Integration of metabolism and virulence by *Clostridium difficile* CodY. *J Bacteriol* 192:5350–5362. <https://doi.org/10.1128/JB.00341-10>.
 28. Shivers RP, Sonenshein AL. 2004. Activation of the *Bacillus subtilis* global regulator CodY by direct interaction with branched-chain amino acids. *Mol Microbiol* 53:599–611. <https://doi.org/10.1111/j.1365-2958.2004.04135.x>.
 29. Handke LD, Shivers RP, Sonenshein AL. 2008. Interaction of *Bacillus subtilis* CodY with GTP. *J Bacteriol* 190:798–806. <https://doi.org/10.1128/JB.01115-07>.
 30. Dineen SS, Villapakkam AC, Nordman JT, Sonenshein AL. 2007. Repression of *Clostridium difficile* toxin gene expression by CodY. *Mol Microbiol* 66:206–219. <https://doi.org/10.1111/j.1365-2958.2007.05906.x>.
 31. Sonenshein AL. 2005. CodY, a global regulator of stationary phase and virulence in Gram-positive bacteria. *Curr Opin Microbiol* 8:203–207. <https://doi.org/10.1016/j.mib.2005.01.001>.
 32. Hendriksen WT, Bootsma HJ, Esteveo S, Hoogenboezem T, de Jong A, de Groot R, Kuipers OP, Hermans PW. 2008. CodY of *Streptococcus pneumoniae*: link between nutritional gene regulation and colonization. *J Bacteriol* 190:590–601. <https://doi.org/10.1128/JB.00917-07>.
 33. Lopez JM, Marks CL, Freese E. 1979. The decrease of guanine nucleotides initiates sporulation of *Bacillus subtilis*. *Biochim Biophys Acta* 587:238–252. [https://doi.org/10.1016/0304-4165\(79\)90357-X](https://doi.org/10.1016/0304-4165(79)90357-X).
 34. Ratnayake-Lecamwasam M, Serror P, Wong K-W, Sonenshein AL. 2001. *Bacillus subtilis* CodY represses early-stationary-phase genes by sensing GTP levels. *Genes Dev* 15:1093–1103. <https://doi.org/10.1101/gad.874201>.
 35. Majerczyk CD, Sadykov MR, Luong TT, Lee C, Somerville GA, Sonenshein AL. 2008. *Staphylococcus aureus* CodY negatively regulates virulence gene expression. *J Bacteriol* 190:2257–2265. <https://doi.org/10.1128/JB.01545-07>.
 36. van Schaik W, Château A, Dillies M-A, Coppée J-Y, Sonenshein AL, Fouet A. 2009. The global regulator CodY regulates toxin gene expression in *Bacillus anthracis* and is required for full virulence. *Infect Immun* 77:4437–4445. <https://doi.org/10.1128/IAI.00716-09>.
 37. Lobel L, Sigal N, Borovok I, Ruppin E, Herskovits AA. 2012. Integrative genomic analysis identifies isoleucine and CodY as regulators of *Listeria monocytogenes* virulence. *PLoS Genet* 8:e1002887. <https://doi.org/10.1371/journal.pgen.1002887>.
 38. Kreth J, Chen Z, Ferretti J, Malke H. 2011. Counteractive balancing of transcriptome expression involving CodY and CovRS in *Streptococcus pyogenes*. *J Bacteriol* 193:4153–4165. <https://doi.org/10.1128/JB.00061-11>.
 39. Boyd CD, O'Toole GA. 2012. Second messenger regulation of biofilm formation: breakthroughs in understanding c-di-GMP effector systems. *Annu Rev Cell Dev Biol* 28:439–462. <https://doi.org/10.1146/annurev-cellbio-101011-155705>.
 40. Hisert KB, MacCoss M, Shiloh MU, Darwin KH, Singh S, Jones RA, Ehrt S, Zhang Z, Gaffney BL, Gandotra S, Holden DW, Murray D, Nathan C. 2005. A glutamate-alanine-leucine (EAL) domain protein of *Salmonella* controls bacterial survival in mice, antioxidant defence and killing of macrophages: role of cyclic diGMP. *Mol Microbiol* 56:1234–1245. <https://doi.org/10.1111/j.1365-2958.2005.04632.x>.
 41. Kulasakara H, Lee V, Brenic A, Liberati N, Urbach J, Miyata S, Lee DG, Neely AN, Hyodo M, Hayakawa Y, Ausubel FM, Lory S. 2006. Analysis of *Pseudomonas aeruginosa* diguanylate cyclases and phosphodiesterases reveals a role for bis-(3'-5')-cyclic-GMP in virulence. *Proc Natl Acad Sci U S A* 103:2839–2844. <https://doi.org/10.1073/pnas.0511090103>.
 42. Tamayo R, Schild S, Pratt JT, Camilli A. 2008. Role of cyclic di-GMP during El Tor biotype *Vibrio cholerae* infection: characterization of the in vivo-induced cyclic di-GMP phosphodiesterase CdpA. *Infect Immun* 76:1617–1627. <https://doi.org/10.1128/IAI.01337-07>.
 43. Tischler AD, Camilli A. 2005. Cyclic diguanylate regulates *Vibrio cholerae* virulence gene expression. *Infect Immun* 73:5873–5882. <https://doi.org/10.1128/IAI.73.9.5873-5882.2005>.
 44. Sun Y-C, Koumoutsis A, Jarrett C, Lawrence K, Gherardini FC, Darby C, Hinnebusch BJ. 2011. Differential control of *Yersinia pestis* biofilm formation *in vitro* and in the flea vector by two c-di-GMP diguanylate cyclases. *PLoS One* 6:e19267. <https://doi.org/10.1371/journal.pone.0019267>.
 45. He M, Zhang J-J, Ye M, Lou Y, Yang XF. 2014. Cyclic Di-GMP receptor PlzA controls virulence gene expression through RpoS in *Borrelia burgdorferi*. *Infect Immun* 82:445–452. <https://doi.org/10.1128/IAI.01238-13>.

46. Purcell EB, Tamayo R. 2016. Cyclic diguanylate signaling in Gram-positive bacteria. *FEMS Microbiol Rev* 40:753–773. <https://doi.org/10.1093/femsre/fuw013>.
47. Ryjenkov DA, Tarutina M, Moskvina OV, Gomelsky M. 2005. Cyclic diguanylate is a ubiquitous signaling molecule in bacteria: insights into biochemistry of the GGDEF protein domain. *J Bacteriol* 187:1792–1798. <https://doi.org/10.1128/JB.187.5.1792-1798.2005>.
48. Schmidt AJ, Ryjenkov DA, Gomelsky M. 2005. The ubiquitous protein domain EAL is a cyclic diguanylate-specific phosphodiesterase: enzymatically active and inactive EAL domains. *J Bacteriol* 187:4774–4781. <https://doi.org/10.1128/JB.187.14.4774-4781.2005>.
49. Ryan RP, Fouhy Y, Lucey JF, Dow JM. 2006. Cyclic di-GMP signaling in bacteria: recent advances and new puzzles. *J Bacteriol* 188:8327–8334. <https://doi.org/10.1128/JB.01079-06>.
50. Galperin MY, Nikolskaya AN, Koonin EV. 2001. Novel domains of the prokaryotic two-component signal transduction systems. *FEMS Microbiol Lett* 203:11–21. <https://doi.org/10.1111/j.1574-6968.2001.tb10814.x>.
51. Galperin MY. 2005. The Molecular Biology Database Collection: 2005 update. *Nucleic Acids Res* 33:D5–24. <https://doi.org/10.1093/nar/gki139>.
52. Sebahia M, Wren BW, Mullany P, Fairweather NF, Minton N, Stabler R, Thomson NR, Roberts AP, Cerdeno-Tarraga AM, Wang H, Holden MT, Wright A, Churcher C, Quail MA, Baker S, Bason N, Brooks K, Chillingworth T, Cronin A, Davis P, Dowd L, Fraser A, Feltwell T, Hance Z, Holroyd S, Jagels K, Moule S, Mungall K, Price C, Rabinowitz E, Sharp S, Simmonds M, Stevens K, Unwin L, Whithead S, Dupuy B, Dougan G, Barrell B, Parkhill J. 2006. The multidrug-resistant human pathogen *Clostridium difficile* has a highly mobile, mosaic genome. *Nat Genet* 38:779–786. <https://doi.org/10.1038/ng1830>.
53. Bordeleau E, Fortier LC, Malouin F, Burrus V. 2011. c-di-GMP turn-over in *Clostridium difficile* is controlled by a plethora of diguanylate cyclases and phosphodiesterases. *PLoS Genet* 7:e1002039. <https://doi.org/10.1371/journal.pgen.1002039>.
54. Gao X, Dong X, Subramanian S, Matthews PM, Cooper CA, Kearns DB, Dann CE. 2014. Engineering of *Bacillus subtilis* strains to allow rapid characterization of heterologous diguanylate cyclases and phosphodiesterases. *Appl Environ Microbiol* 80:6167–6174. <https://doi.org/10.1128/AEM.01638-14>.
55. Purcell EB, McKee RW, McBride SM, Waters CM, Tamayo R. 2012. Cyclic diguanylate inversely regulates motility and aggregation in *Clostridium difficile*. *J Bacteriol* 194:3307–3316. <https://doi.org/10.1128/JB.00100-12>.
56. Soutourina OA, Monot M, Boudry P, Saujet L, Pichon C, Sismeiro O, Semenova E, Severinov K, Le Bouguenec C, Coppee JY, Dupuy B, Martin-Verstraete I. 2013. Genome-wide identification of regulatory RNAs in the human pathogen *Clostridium difficile*. *PLoS Genet* 9:e1003493. <https://doi.org/10.1371/journal.pgen.1003493>.
57. McKee RW, Mangalea MR, Purcell EB, Borchardt EK, Tamayo R. 2013. The second messenger cyclic di-GMP regulates *Clostridium difficile* toxin production by controlling expression of *sigD*. *J Bacteriol* 195:5174–5185. <https://doi.org/10.1128/JB.00501-13>.
58. El Meouche I, Peltier J, Monot M, Soutourina O, Pestel-Caron M, Dupuy B, Pons J-L. 2013. Characterization of the SigD regulon of *C. difficile* and its positive control of toxin production through the regulation of *tcdR*. *PLoS One* 8:e83748. <https://doi.org/10.1371/journal.pone.0083748>.
59. Bordeleau E, Purcell EB, Lafontaine DA, Fortier LC, Tamayo R, Burrus V. 2015. Cyclic di-GMP riboswitch-regulated type IV pili contribute to aggregation of *Clostridium difficile*. *J Bacteriol* 197:819–832. <https://doi.org/10.1128/JB.02340-14>.
60. Purcell EB, McKee RW, Bordeleau E, Burrus V, Tamayo R. 2015. Regulation of type IV pili contributes to surface behaviors of historical and epidemic strains of *Clostridium difficile*. *J Bacteriol* 198:565–577. <https://doi.org/10.1128/JB.00816-15>.
61. Peltier J, Shaw HA, Couchman EC, Dawson LF, Yu L, Choudhary JS, Kaefer V, Wren BW, Fairweather NF. 2015. Cyclic diGMP regulates production of sortase substrates of *Clostridium difficile* and their surface exposure through ZmpI protease-mediated cleavage. *J Biol Chem* 290:24453–24469. <https://doi.org/10.1074/jbc.M115.665091>.
62. Cafardi V, Biagini M, Martinelli M, Leuzzi R, Rubino JT, Cantini F, Norais N, Scarselli M, Serruto D, Unnikrishnan M. 2013. Identification of a novel zinc metalloprotease through a global analysis of *Clostridium difficile* extracellular proteins. *PLoS One* 8:e81306. <https://doi.org/10.1371/journal.pone.0081306>.
63. Hensbergen PJ, Klychnikov OI, Bakker D, Dragan I, Kelly ML, Minton NP, Corver J, Kuijper EJ, Drijfhout JW, van Leeuwen HC. 2015. *Clostridium difficile* secreted Pro-Pro endopeptidase PPEP-1 (ZMP1/CD2830) modulates adhesion through cleavage of the collagen binding protein CD2831. *FEMS Lett* 589:3952–3958. <https://doi.org/10.1016/j.femslet.2015.10.027>.
64. Henry JT, Crosson S. 2011. Ligand-binding PAS domains in a genomic, cellular, and structural context. *Annu Rev Microbiol* 65:261–286. <https://doi.org/10.1146/annurev-micro-121809-151631>.
65. Christen M, Christen B, Folcher M, Schauer A, Jenal U. 2005. Identification and characterization of a cyclic di-GMP-specific phosphodiesterase and its allosteric control by GTP. *J Biol Chem* 280:30829–30837. <https://doi.org/10.1074/jbc.M504429200>.
66. Kazmierczak BI, Lebron MB, Murray TS. 2006. Analysis of FimX, a phosphodiesterase that governs twitching motility in *Pseudomonas aeruginosa*. *Mol Microbiol* 60:1026–1043. <https://doi.org/10.1111/j.1365-2958.2006.05156.x>.
67. An S, Wu Je Zhang L-H. 2010. Modulation of *Pseudomonas aeruginosa* biofilm dispersal by a cyclic-di-GMP phosphodiesterase with a putative hypoxia-sensing domain. *Appl Environ Microbiol* 76:8160–8173. <https://doi.org/10.1128/AEM.01233-10>.
68. Enomoto G, Ni Ni W, Narikawa R, Ikeuchi M. 2015. Three cyanobacteriochromes work together to form a light color-sensitive input system for c-di-GMP signaling of cell aggregation. *Proc Natl Acad Sci U S A* 112:8082–8087. <https://doi.org/10.1073/pnas.1504228112>.
69. Chan C, Paul R, Samoray D, Amiot NC, Giese B, Jenal U, Schirmer T. 2004. Structural basis of activity and allosteric control of diguanylate cyclase. *Proc Natl Acad Sci U S A* 101:17084–17089. <https://doi.org/10.1073/pnas.0406134101>.
70. Wassmann P, Chan C, Paul R, Beck A, Heerklotz H, Jenal U, Schirmer T. 2007. Structure of BeF₃-modified response regulator PleD: implications for diguanylate cyclase activation, catalysis, and feedback inhibition. *Structure* 15:915–927. <https://doi.org/10.1016/j.str.2007.06.016>.
71. Navarro MV, De N, Bae N, Wang Q, Sondermann H. 2009. Structural analysis of the GGDEF-EAL domain-containing c-di-GMP receptor FimX. *Structure* 17:1104–1116. <https://doi.org/10.1016/j.str.2009.06.010>.
72. Đapa T, Leuzzi R, Ng YK, Baban ST, Adamo R, Kuehne SA, Scarselli M, Minton NP, Serruto D, Unnikrishnan M. 2013. Multiple factors modulate biofilm formation by the anaerobic pathogen *Clostridium difficile*. *J Bacteriol* 195:545–555. <https://doi.org/10.1128/JB.01980-12>.
73. Saujet L, Monot M, Dupuy B, Soutourina O, Martin-Verstraete I. 2011. The key sigma factor of transition phase, SigH, controls sporulation, metabolism, and virulence factor expression in *Clostridium difficile*. *J Bacteriol* 193:3186–3196. <https://doi.org/10.1128/JB.00272-11>.
74. Heap JT, Pennington OJ, Cartman ST, Carter GP, Minton NP. 2007. The CloStron: a universal gene knock-out system for the genus *Clostridium*. *J Microbiol Methods* 70:452–464. <https://doi.org/10.1016/j.mimet.2007.05.021>.
75. Faulds-Pain A, Wren BW. 2013. Improved bacterial mutagenesis by high-frequency allele exchange, demonstrated in *Clostridium difficile* and *Streptococcus suis*. *Appl Environ Microbiol* 79:4768–4771. <https://doi.org/10.1128/AEM.01195-13>.
76. Martin-Verstraete I, Peltier J, Dupuy B. 2016. The regulatory networks that control *Clostridium difficile* toxin synthesis. *Toxins (Basel)* 8:E153. <https://doi.org/10.3390/toxins8050153>.
77. Miura M, Kato H, Matsushita O. 2011. Identification of a novel virulence factor in *Clostridium difficile* that modulates toxin sensitivity of cultured epithelial cells. *Infect Immun* 79:3810–3820. <https://doi.org/10.1128/IAI.00051-11>.
78. Riedl J, Crevenna AH, Kessenbrock K, Yu JH, Neukirchen D, Bista M, Bradke F, Jenne D, Holak TA, Werb Z, Sixt M, Wedlich-Soldner R. 2008. Lifeact: a versatile marker to visualize F-actin. *Nat Methods* 5:605. <https://doi.org/10.1038/nmeth.1220>.
79. Christen B, Christen M, Paul R, Schmid F, Folcher M, Jenoe P, Meuwly M, Jenal U. 2006. Allosteric control of cyclic di-GMP signaling. *J Biol Chem* 281:32015–32024. <https://doi.org/10.1074/jbc.M603589200>.
80. Schultz J, Milpetz F, Bork P, Ponting CP. 1998. SMART, a simple modular architecture research tool: identification of signaling domains. *Proc Natl Acad Sci U S A* 95:5857–5864. <https://doi.org/10.1073/pnas.95.11.5857>.
81. Chiaverotti TA, Parker G, Gallant J, Agabian N. 1981. Conditions that trigger guanosine tetraphosphate accumulation in *Caulobacter crescentus*. *J Bacteriol* 145:1463–1465.
82. Ochi K. 1987. Metabolic initiation of differentiation and secondary metabolism by *Streptomyces griseus*: significance of the stringent response (ppGpp) and GTP content in relation to A factor. *J Bacteriol* 169:3608–3616. <https://doi.org/10.1128/jb.169.8.3608-3616.1987>.
83. Whitehead KE, Webber GM, England RR. 1998. Accumulation of ppGpp

- in *Streptococcus pyogenes* and *Streptococcus rattus* following amino acid starvation. FEMS Microbiol Lett 159:21–26. <https://doi.org/10.1111/j.1574-6968.1998.tb12836.x>.
84. Inaoka T, Ochi K. 2002. RelA protein is involved in induction of genetic competence in certain *Bacillus subtilis* strains by moderating the level of intracellular GTP. J Bacteriol 184:3923–3930. <https://doi.org/10.1128/JB.184.14.3923-3930.2002>.
 85. Belitsky BR, Brinsmade SR, Sonenshein AL. 2015. Intermediate levels of *Bacillus subtilis* CodY activity are required for derepression of the branched-chain amino acid permease, BraB. PLoS Genet 11:e1005600. <https://doi.org/10.1371/journal.pgen.1005600>.
 86. Waters NR, Samuels DJ, Behera RK, Livny J, Rhee KY, Sadykov MR, Brinsmade SR. 2016. A spectrum of CodY activities drives metabolic reorganization and virulence gene expression in *Staphylococcus aureus*. Mol Microbiol 101:495–514. <https://doi.org/10.1111/mmi.13404>.
 87. Buckstein MH, He J, Rubin H. 2008. Characterization of nucleotide pools as a function of physiological state in *Escherichia coli*. J Bacteriol 190:718–726. <https://doi.org/10.1128/JB.01020-07>.
 88. Newell PD, Monds RD, O'Toole GA. 2009. LapD is a bis-(3',5')-cyclic dimeric GMP-binding protein that regulates surface attachment by *Pseudomonas fluorescens* Pf0-1. Proc Natl Acad Sci U S A 106:3461–3466. <https://doi.org/10.1073/pnas.0808933106>.
 89. Gjermansen M, Nilsson M, Yang L, Tolker-Nielsen T. 2010. Characterization of starvation-induced dispersion in *Pseudomonas putida* biofilms: genetic elements and molecular mechanisms. Mol Microbiol 75:815–826. <https://doi.org/10.1111/j.1365-2958.2009.06793.x>.
 90. Bharati BK, Sharma IM, Kasetty S, Kumar M, Mukherjee R, Chatterji D. 2012. A full-length bifunctional protein involved in c-di-GMP turnover is required for long-term survival under nutrient starvation in *Mycobacterium smegmatis*. Microbiology 158:1415–1427. <https://doi.org/10.1099/mic.0.053892-0>.
 91. Nguyen D, Joshi-Datar A, Lepine F, Bauerle E, Olakanmi O, Beer K, McKay G, Siehnel R, Schafhauser J, Wang Y, Britigan BE, Singh PK. 2011. Active starvation responses mediate antibiotic tolerance in biofilms and nutrient-limited bacteria. Science 334:982–986. <https://doi.org/10.1126/science.1211037>.
 92. Hooper LV, Midtvedt T, Gordon JI. 2002. How host-microbial interactions shape the nutrient environment of the mammalian intestine. Annu Rev Nutr 22:283–307. <https://doi.org/10.1146/annurev.nutr.22.011602.092259>.
 93. Ng SC, Lam EF, Lam TT, Chan Y, Law W, Tse PC, Kamm MA, Sung JJ, Chan FK, Wu JC. 2013. Effect of probiotic bacteria on the intestinal microbiota in irritable bowel syndrome. J Gastroenterol Hepatol 28:1624–1631. <https://doi.org/10.1111/jgh.12306>.
 94. Ternan NG, Jain S, Srivastava M, McMullan G. 2012. Comparative transcriptional analysis of clinically relevant heat stress response in *Clostridium difficile* strain 630. PLoS One 7:e42410. <https://doi.org/10.1371/journal.pone.0042410>.
 95. Osorio CG, Crawford JA, Michalski J, Martinez-Wilson H, Kaper JB, Camilli A. 2005. Second-generation recombination-based in vivo expression technology for large-scale screening for *Vibrio cholerae* genes induced during infection of the mouse small intestine. Infect Immun 73:972–980. <https://doi.org/10.1128/IAI.73.2.972-980.2005>.
 96. Yanisch-Perron C, Vieira J, Messing J. 1985. Improved M13 phage cloning vectors and host strains: nucleotide sequences of the M13mp18 and pUC19 vectors. Gene 33:103–119. [https://doi.org/10.1016/0378-1119\(85\)90120-9](https://doi.org/10.1016/0378-1119(85)90120-9).
 97. Lyras D, Rood JI. 1998. Conjugative transfer of RP4-oriT shuttle vectors from *Escherichia coli* to *Clostridium perfringens*. Plasmid 39:160–164. <https://doi.org/10.1006/plas.1997.1325>.
 98. McBride SM, Sonenshein AL. 2011. Identification of a genetic locus responsible for antimicrobial peptide resistance in *Clostridium difficile*. Infect Immun 79:167–176. <https://doi.org/10.1128/IAI.00731-10>.
 99. Fuller JR, Vitko NP, Perkowski EF, Scott E, Khatri D, Spontak JS, Thurlow LR, Richardson AR. 2011. Identification of a lactate-quinone oxidoreductase in *Staphylococcus aureus* that is essential for virulence. Front Cell Infect Microbiol 1:19. <https://doi.org/10.3389/fcimb.2011.00019>.
 100. Gasteiger J. 2006. Chemoinformatics: a new field with a long tradition. Anal Bioanal Chem 384:57–64. <https://doi.org/10.1007/s00216-005-0065-y>.
 101. Pratt JT, Tamayo R, Tischler AD, Camilli A. 2007. PilZ domain proteins bind cyclic diguanylate and regulate diverse processes in *Vibrio cholerae*. J Biol Chem 282:12860–12870. <https://doi.org/10.1074/jbc.M611593200>.
 102. Tamayo R, Tischler AD, Camilli A. 2005. The EAL domain protein VieA is a cyclic diguanylate phosphodiesterase. J Biol Chem 280:33324–33330. <https://doi.org/10.1074/jbc.M506500200>.
 103. Kariisa AT, Grube A, Tamayo R. 2015. Two nucleotide second messengers regulate the production of the *Vibrio cholerae* colonization factor GbpA. BMC Microbiol 15:166. <https://doi.org/10.1186/s12866-015-0506-5>.
 104. Garnier T, Cole ST. 1986. Characterization of a bacteriocinogenic plasmid from *Clostridium perfringens* and molecular genetic analysis of the bacteriocin-encoding gene. J Bacteriol 168:1189–1196. <https://doi.org/10.1128/jb.168.3.1189-1196.1986>.
 105. Choi W, Acharya BR, Peyret G, Fardin MA, Mege RM, Ladoux B, Yap AS, Fanning AS, Peifer M. 2016. Remodeling the zonula adherens in response to tension and the role of afadin in this response. J Cell Biol 213:243–260. <https://doi.org/10.1083/jcb.201506115>.